Journal of Asian Concrete Federation
Vol. 4, No. 1, pp. 1-11, June 2018
ISSN 2465-7964 / eISSN 2465-7972
https://doi.org/10.18702/acf.2018.07.3.1.1

Technical Paper

Proposal of a fatigue life prediction method for RC slabs failed under traveling wheel-type load test

Kyoko TAKEDA*, Natsuko HAMADA and Yasuhiko SATO

(Received: June 27, 2017; Accepted: April 30, 2018; Published online: July 03, 2018)

Abstract: Reinforced concrete (RC) bridge deck slabs are major components of a bridge superstructure, and RC slabs are usually damaged under fatigue loading and fail in shear. In order to solve this problem, many researchers performed numerous experiments and investigations over past decades. These efforts indicate that punching shear failure mode observed in real bridges can be simulated by a traveling wheel-type load test. To date, researchers developed several fatigue life prediction methods and proposed failure mechanisms based on the experimental results performed in past studies. However, experimental results indicate different trends, because the fatigue life of RC slabs is affected by various factors. Therefore, there is a need for a rational fatigue life prediction method that can inclusively evaluate all experimental results from past studies. It is important to note that a prediction method based on damage and failure mechanism under fatigue loading has not been developed to date. In the present study, a fatigue life prediction method that was developed based on the existing experimental data of fatigue life of RC slabs is proposed by modifying the JSCE shear design equation for a linear member. In the method, reinforcement ratios of both main and distributing bars and the proportion between main and distributing bars are considered as major parameters because slabs are modeled as beam-formed elements when traveling load is applied. In the study, the sensitivity of reinforcement ratios toward fatigue life in each method is compared: the proposed method, 3D Finite Element (FE) analysis, and an existing equation by Matsui. The results indicate that the proposed equation estimates greater effects of the reinforcement when compared to the existing equation and FE analysis.

Keywords: RC slabs, fatigue life prediction, 3D FEM, traveling wheel-type load, reinforcement ratio.

1. Introduction

Bridge maintenance for service life extension is a significant social issue. A key technology for conducting proper maintenance corresponds to precisely predicting the exact time when bridges should be repaired, strengthened or renewed based on reasonable prediction. The proper maintenance requires assessing precise residual strength of members and their service life. Fatigue failure in RC members is a serious problem and continues to be actively investigated [1,2]. More specifically, reinforced concrete slabs (RC slabs) in bridges are often damaged by fatigue loading, and thus, it is imperative to establish clear failure mechanisms and establish prediction methods for fatigue life. This study involves examining the fatigue life of RC slabs under traveling wheel-type loads.

As it is well known from the past studies, the typical failure mode of RC slabs corresponds to punching shear failure that is a failure mode in which concrete compression zone under a loading point are punched and failed [3-6]. Several studies focused on clarifying the aforementioned fatigue damage observed in RC slabs. Kakuta et al. performed a fixed-point fatigue load test for RC slabs and examined the mechanism of punching shear failure [5,6]. Matsui indicated that the actual failure mode observed in real road bridges differs from the failure mode observed in a fixed-point fatigue load test, and this type of behavior is observed in a traveling wheel-type load test [4]. Thus, to date, several traveling wheel-type load tests were reported, and various methods to predict fatigue life were proposed by some researchers including Abe [7,8] and Maeshima [9]. The most widely known prediction

Corresponding author K. Takeda is a Ph.D. student, Graduate School of Creative Science and Engineering, Waseda University, Tokyo, Japan.
N. Hamada is a Scientific Officer of Research Institute, Kajima Corporation, Tokyo, Japan.
Y. Sato is a Professor, Department of Civil and Environmental Engineering, Waseda University, Tokyo, Japan.

method in Japan was developed by Matsui [10]. Although several experimental studies were continuously performed, analytical investigations using three-dimensional nonlinear finite element analysis (3D-FEA) were only conducted recently [11-15].

However, experimental studies performed by different institutes reveal different trends, because the specimens possess a wide range of slab sizes and wheel-loads. The fatigue life of RC slabs is affected by various factors, and thus, a rational fatigue life prediction method that inclusively evaluates all experimental results from past studies has not been proposed to date. Given this issue, in previous studies authors developed fatigue life prediction methods based on experimentally observed fatigue life. The present study proposes a method to evaluate the influences of main and distributing bars on fatigue life by performing a comparative investigation of the proposed method by authors, an existing equation by Matsui [10], and 3D FEA results.

2. Fatigue life prediction method for RC slabs

2.1 Experimental data used

Based on past experiments, a new fatigue life prediction method was developed. In this study, experimental data from 93 slabs that failed under a traveling wheel-type loading test with a constant load [16] were collected. The slabs included dimensional data in the following range: 70–220 mm thickness, main reinforcement ratio within 0.74–1.74 %, distributing reinforcement ratio within 0.26–1.41 %, and compressive strength within 13.6–54.0 MPa.

2.2 Modeling of RC slabs based on the failure mechanism

Past studies indicated that RC slabs under a traveling wheel-type load test show shear failure like a beam in the main reinforcement direction [4]. With the aim of seamless connectivity between the shear design of linear members and that of plate members, a shear strength equation for the slabs under a traveling wheel-type loading is constructed in this study based on the shear strength equation for a linear member such as beam and column. The flowing JSCE shear design equation for a linear member [17] is adapted in this study.

$$V_{cd} = \beta_d \cdot \beta_p \cdot f_{vcd} \cdot b_w \cdot d \ \text{(N)} \qquad (1)$$

where, $f_{vcd} = 0.20\sqrt[3]{f'_{cd}}$, $\beta_d = \sqrt[4]{1000/d}$, $\beta_p = \sqrt[3]{100p}$, f'_{cd} denotes the compressive strength (N/mm^2), d denotes the effective depth of the main reinforcement (mm), p denotes the main reinforcement ratio, and b_w denotes the width of a beam (mm).

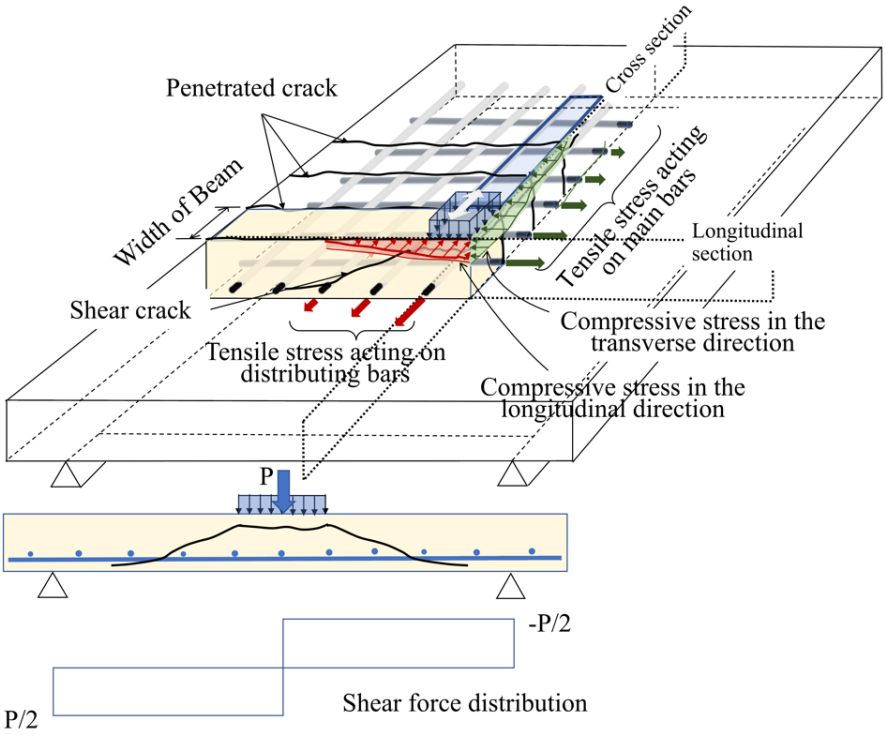

Fig. 1 – Conceptual stress state in the cracked RC slab

The conceptual stress state in an RC slab is shown in Fig.1. With respect to a traveling wheel-type load, the RC slab is gradually damaged, and penetrated cracks occur in the transverse direction. Subsequently, the slab resembles a few beams placed in a line linked with only distributing bars. This type of a damaged slab is termed as "beam-formed." A beam-formed member may be under a biaxial stress state. Compressive stress in upper part of RC slab by balancing with tensile stress of main and distributing reinforcement (transverse reinforcement) act on the cross-section of longitudinal and transverse directions as shown in Fig.1. There is a significant difference between the linear member and beam-formed member.

An important issue corresponds to a method to determine the width of the beam-formed member *B*. In this study, Eq. (2) proposed by Matsui [11] is adapted.

$$B = b + 2d_d \text{ (mm)} \quad (2)$$

where, *b* denotes the loading plate length in the longitudinal direction (wheel-travel direction) (mm), and d_d denotes the effective depth of the distributing reinforcement (mm).

2.3 Proposed fatigue life prediction method

In the proposed method, the shear strength equation for beam-formed member is developed. In section 2.2, it was described that the beam-formed member might be under a biaxial stress state because of both main and distributing reinforcement acting on the cross-section of longitudinal and transverse directions. There is a significant difference between the linear member and the beam-formed member: in other words, to predict precisely fatigue life of RC slabs, JSCE shear design equation Eq. (1) should be modified to consider the influence of both main and distributing reinforcement. Accordingly, based on experimental results of 93 slabs as 2.1 section shows, authors developed a new equation by modifying Eq. (1). The new equation can consider the influences of distributing reinforcement additionally. At first, authors decided to introduce new terms β_{p1} and β_{p2} included in Eq. (3) in which main and distributing reinforcement ratio affect each other. Then, authors decided a value of term which expresses the influence of reinforcement to aim at the minimum scattering for predicting fatigue life of many experimental results. The developed equation is expressed as follows:

$$V_{bc} = \alpha_e \cdot \beta_{p1} \cdot \beta_{p2} \cdot \beta_d \cdot f_{vmcd} \cdot b_{w\_e} \cdot d \text{ (N)} \quad (3)$$

where, α_e denotes the coefficient for a moisture state as follows: 1.0 in the dry condition and 0.69 in the wet condition, β_{p1} denotes the influence of main reinforcement, and β_{p2} denotes the influence of distributing reinforcement.

The expressions are as follows:

$$\beta_{p1} = (100p_1)^{\left\{\frac{1}{3}+0.5(100p_2)\right\}} \quad (4)$$

$$\beta_{p2} = 1 + 0.125\frac{p_2}{p_1} \quad (5)$$

where, $f_{vmcd} = 0.32\sqrt[3]{f'_{cd}}$, b_{w_e} denotes the width of a beam-formed member calculated by Eq. (2) (mm), p_1 denotes the main reinforcement ratio, and p_2 denotes the distributing reinforcement ratio.

Figure 2 shows the relationship between the experimentally observed fatigue life *N* and applied force normalized by twice that of V_{bc} calculated by Eq. (3). V_{bc} should be doubled because the load acts at the center of the span in the experiment. In both dry and wet conditions, fatigue life linearly decreases from *S* = 1.0. All the experimental data from past studies by some research institutes were uniformly dispersed around the solid and broken lines.

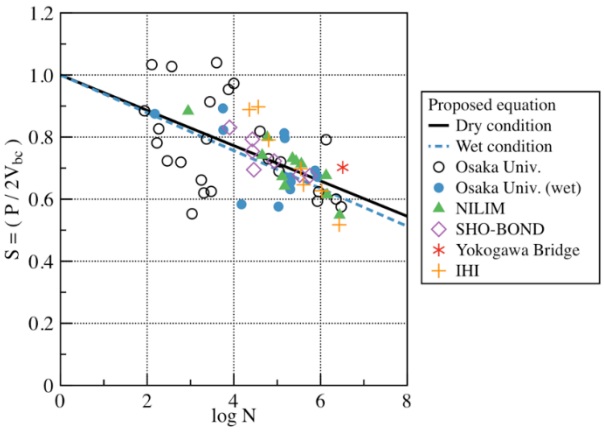

Fig. 2 – S–N curves from the proposed method and experimental results

The relationship between *S* and *N* is expressed as follows:

$$S = \frac{P}{2V_{bc}} = 1 - KlogN \quad (6)$$

where, *K* = 0.057 in the dry condition, *K* = 0.061 in the wet condition, and N denotes the number of cyclic loadings.

Figures 3 through 5 illustrate the relationships between the ratio of S_{cal} to S_{exp} and major parameters including the main reinforcement ratio, distributing reinforcement ratio, and compressive strength, respectively. Specifically, S_{cal} is S derived from Eq. (6) by substituting the fatigue life observed in the experiment, and S_{exp} is the ratio of the applied force in the experiment to the shear strength calculated using Eqs. (2) - (5). The proposed method properly estimates the influence of major parameters because the ratio of S_{cal} to S_{exp} is distributed at approximately 1.0, irrespective of the parameters.

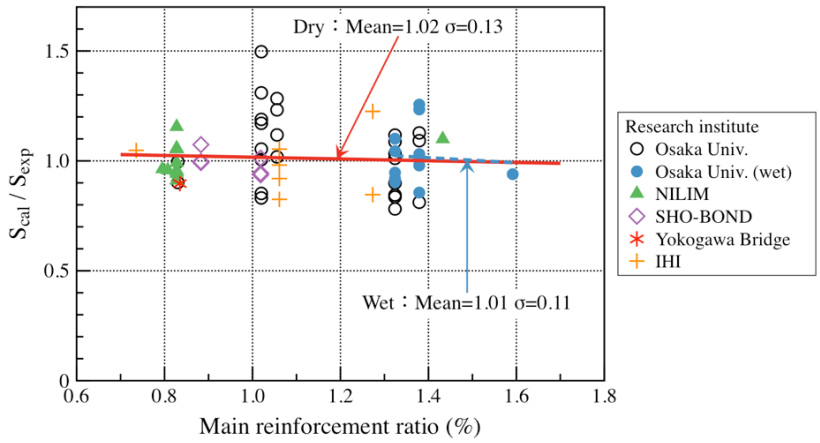

Fig. 3 – Influence of the main reinforcement ratio in the proposed method

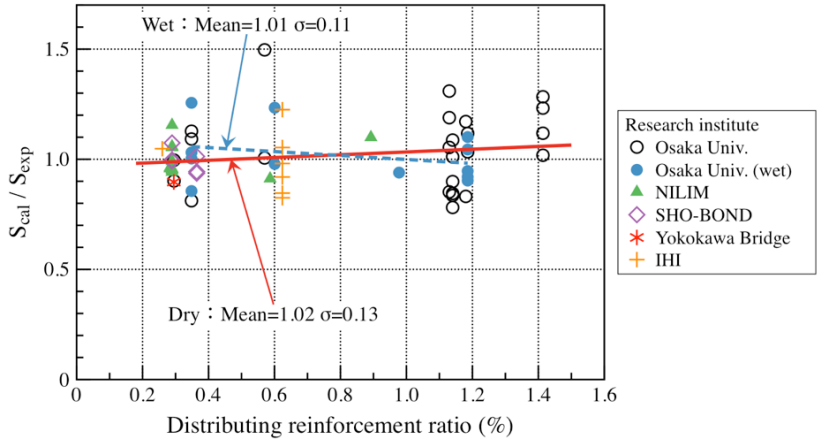

Fig. 4 – Influence of the distributing reinforcement ratio in the proposed method

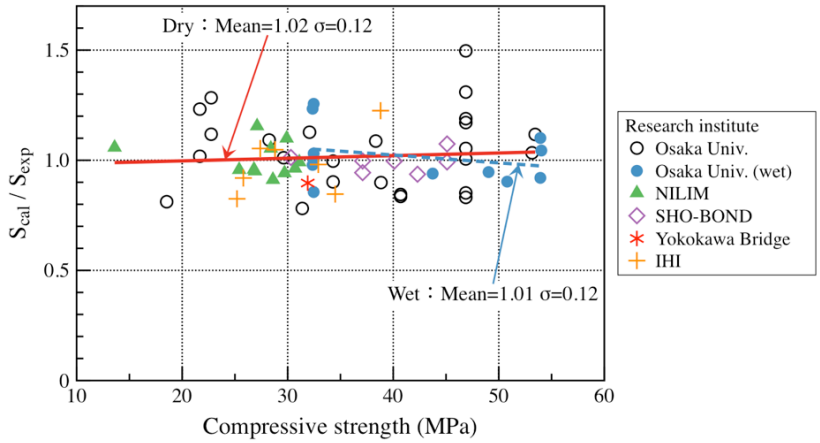

Fig. 5 – Influence of compressive strength in the proposed method

3. Three-dimensional FE analysis

3.1 Analytical overview and finite element modeling

In the three-dimensional analytical investigation, DuCOM-COM3 developed at the University of Tokyo is used. This program contains tension and compression models and a shear transfer model in cracked concrete. The program simulates the fatigue damage process due to cyclic loading using path-dependent high-cycle fatigue modeling [12]. It is considered that plastic deformation increments and stiffness reduction based on time explain the fatigue damage process. In order to prepare analysis models, past studies referred to the specimen size of the traveling wheel-type loading test performed by the National Institute for Land and Infrastructure Management (NILIM) [16]. Figure 6 shows the finite element mesh used in the analysis, and Table 1 gives the details of the slabs. The slab was simply supported in the longitudinal direction and elastically supported with steel girders in the transverse direction. In the analysis, a simple support in both directions was applied owing to difficulties in modeling the elastic support. Steel plates were prepared in the support to prevent local failure caused by the impact force. A wheel-load was directly applied on the nodal points at the center of the slab model along the length of 3,000 mm in the longitudinal direction with a width of 500 mm as shown in Fig. 6.

3.2 Definition of fatigue life in the analysis

Figure 7 shows the relationship between the logarithm of the number of cyclic loadings and deflection at the center of the slab for different applied loads. In all the cases, the deflection rapidly increased after approximately 10,000 cycles. An increase in the wheel-load increases the initial deflection and decreases the fatigue life with the exception of specimen RC39-3. Specimen RC39-3 exhibited significantly higher deflection although the applied wheel-load is the lowest among the specimens because the compressive strength of RC39-3 was approximately 50% of the other specimens.

The number of cycles at failure is an important index while considering fatigue durability. However, it is difficult to define fatigue failure in the analysis [13] as the FE analysis (FEA) continues steady calculations despite the occurrence of a significant increase in deflection. In the study, the change in the reaction force on the support is especially noted because severe damage that induces fatigue failure potentially affects the internal loading path.

Figure 8 shows the reaction force distribution observed in specimen RC39-7 on the longitudinal supporting line when the wheel load was located at the center of span. In the figure, the horizontal axis, vertical axis, and depth axis show the location in the longitudinal direction, reaction force at each node, and number of cycles, respectively. The shape of the distribution is similar to that of a mountain in which a higher reaction force is observed around the center. Nevertheless, with respect to approximately 15,000 cycles, it was observed that the top of the mountain-shape gradually declines, and the reaction force appears to shift to the left and right edges. The reaction force at the center exhibited the lowest value at approximately 140,000 cycles.

Table 1 – Details of the analyzed RC slabs

Specimen	Compressive strength (MPa)	Tensile strength (MPa)	Elastic modulus (MPa)	Main reinforcing bar	Distributing reinforcing bar	Wheel-load (kN)
RC39-3	13.6	1.44	1.62×10^4	Tension D16 @ 150 Compression D16 @ 300	Tension D13 @ 300 Compression D10 @ 300	105
RC39-4	29.7	2.69	2.39×10^4			196
RC39-5	31.1	2.49	2.34×10^4			167
RC39-7	25.4	2.15	2.39×10^4			152
RC39-8	27.1	2.42	2.32×10^4			118
RC39-9	26.6	2.34	2.68×10^4			157

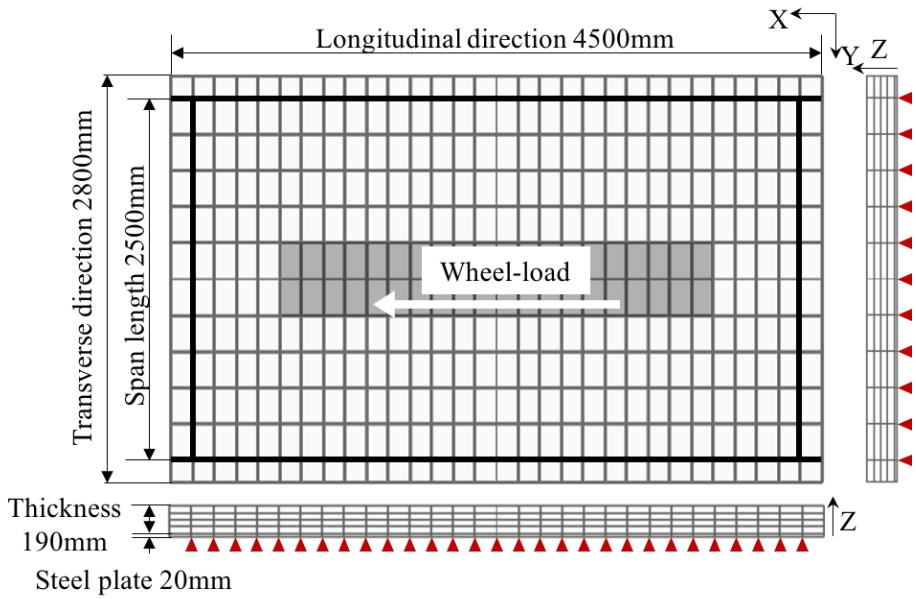

Fig. 6 – Finite element mesh

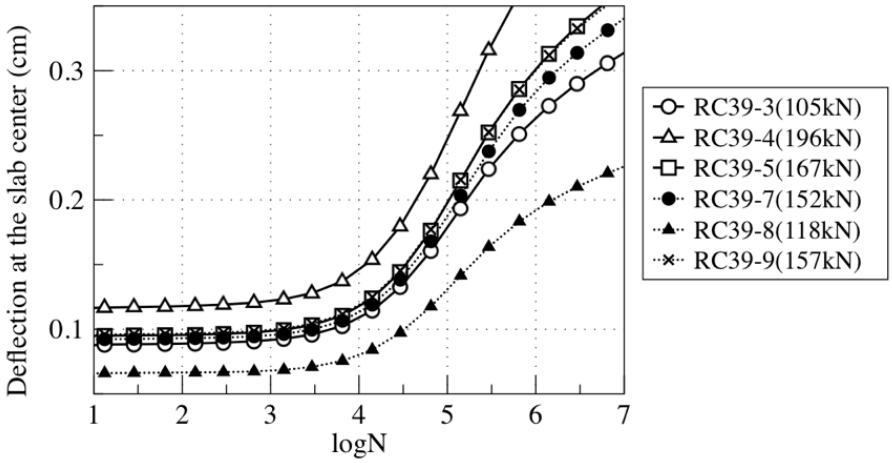

Fig. 7 – Deflection at the center of slab

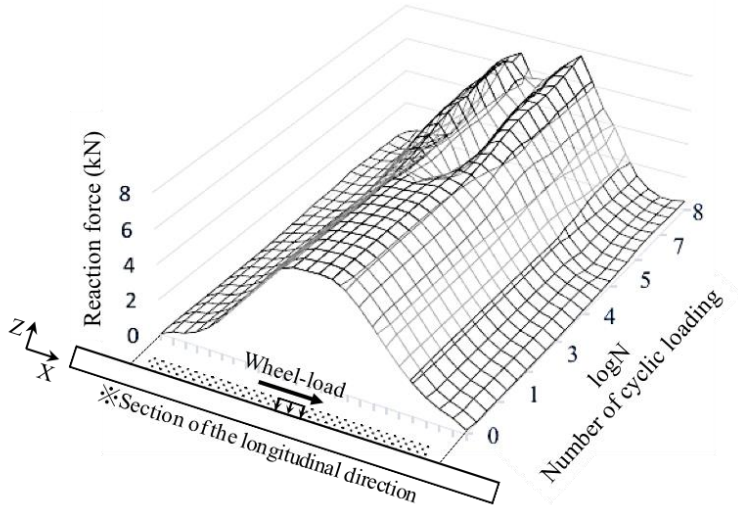

Fig. 8 – Variation in the reaction force distributions in the longitudinal direction

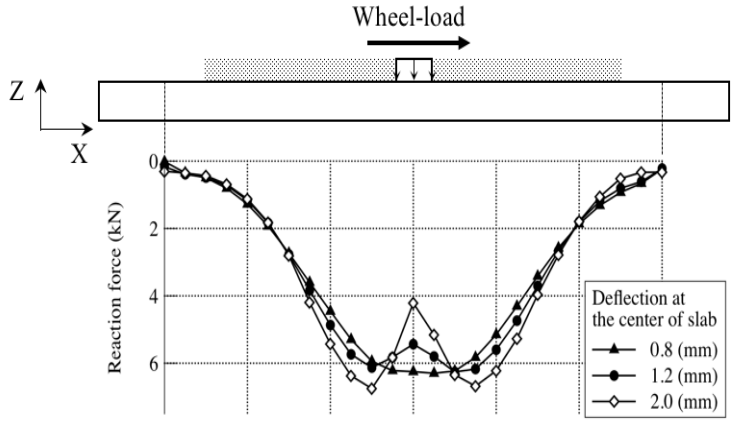

Fig. 9 – Reaction force distributions at different mid-span deflections

A decrease in the reaction force at the node around the center may indicate the development of severe damage in the slab that causes a significant change in the resisting mechanism. Therefore, it is considered that fatigue failure occurs at the point of time when the reaction force decreases. Figure 9 shows the reaction force distributions at mid-span deflections of 0.8 mm, 1.2 mm, and 2.0 mm. The reaction force commenced decreasing when the deflection at the center reached approximately 1.2 mm. The lowest value of the reaction force occurred when the deflection reached approximately 2.0 mm. A similar tendency was observed in all cases, and thus, we define that fatigue failure occurs at a deflection of 2.0 mm in the slabs used in the analysis.

4. Assessing the influence of reinforcement on the fatigue life

A comparison with an existing equation and FEA results is necessary to understand the essential characteristics of the proposed method. This chapter discusses the influences of main and distributing reinforcement on fatigue life. Specifically, the shear strength calculated by the proposed method and the existing equation developed by Matsui [10] [18] are first compared, and the fatigue life derived from each method is then compared.

4.1 Matsui's equation

Several punching shear strength equations for evaluating fatigue life were proposed by past studies. Matsui proposed a prediction equation for the width of a beam-formed member as given in Eq. (2) and punching shear strength P_{sx} as given in Eq. (7) for the beam-formed RC slabs. The S–N curve of the traveling wheel-type load test is also proposed in [18] as Eq. (8). The expressions are as follows:

$$P_{sx} = 2B(f_v x_m + f_t C_m) \quad (7)$$

where, B denotes the width of beam-formed member calculated by Eq. (2) (mm), f_v denotes the shear strength of concrete (N/mm^2), f_t denotes the tensile strength of concrete (N/mm^2), x_m denotes the neutral axis depth of the vertical section for main reinforcement ignoring tension bars (mm), C_m denotes the neutral axis depth of the tension bars (mm).

The fatigue life prediction equation is as follows:

$$\log\left(\frac{P}{P_{sx}}\right) = -0.07835 \log N + \log 1.52 \quad (8)$$

Figures 10 and 11 show the shear strength of the beam-formed RC slabs calculated by the proposed equation (Eq. (3)) and Matsui's equation (Eq. (7)) for different main and distributing reinforcement ratios. As shown in Fig.10, two curves of Matsui's equation that exhibit different distributing reinforcement ratios completely overlap because Matsui's equation does not consider the effect of the distributing bars. The effect of the main reinforcement ratio is higher with respect to increasing the shear strength in both equations. The proposed equation shows the feature in which the presence of distributing reinforcement enhances the effect of the main reinforcement. As shown in Fig.11, the distributing reinforcement ratio affects the shear strength for the proposed equation. An increase in the main reinforcement ratio increases the enhancement effect of the distributing reinforcement ratio for the proposed equation. In contrast, Matsui's equation does not consider the effect of distributing reinforcement. Therefore, the shear strength remains unchanged irrespective of the distributing reinforcement ratio.

4.2 Comparison of fatigue life

Fatigue life from experimental results and the FEA result is compared in Fig.12. Almost all calculated results by the FEA is around logN=5. They have slight difference in fatigue life although their compressive strength and wheel-loads is different as Table.1 shows. The S–N diagram derived from the proposed method, Matsui's equation, and 3D FEA is shown in Fig. 13. The *S* in FEA denotes the value normalized by the shear strength calculated using the proposed method in Eq. (3). Two S–N curves obtained using the proposed method and Matsui's equation cross each other at approximately *S* =0.8. Thus, Matsui's equation predicts a longer fatigue life when compared to that of the proposed method in the range exceeding *S* =0.8 while the proposed method calculates longer fatigue life in the range under *S* =0.8. However, a plot at *S* =0.88 exceeds the S–N curve and the FEA estimates a considerably higher fatigue life when compared to the proposed method. Therefore, to expand the range of *S* considered, additional analyses were performed in the case of *S* =0.95 and 0.5, and two data plots were added in Fig. 13. The result of *S* =0.5 was plotted slightly below the S–N curve. However, it agreed well with the proposed method. Conversely, with respect to the case of *S* =0.95, almost 30,000 cycles up to failure are required although the wheel-load was nearly equal to its shear strength. The reason as to why FEA is unable to accurately simulate the low cycle fatigue failure is due to differences in the failure mode between low-cycle and high-cycle loadings and the definition of fatigue failure such that it fails at the mid-span deflection of 2.0 mm, which is not applicable to low cycle fatigue failure. This remains as an issue that should be addressed.

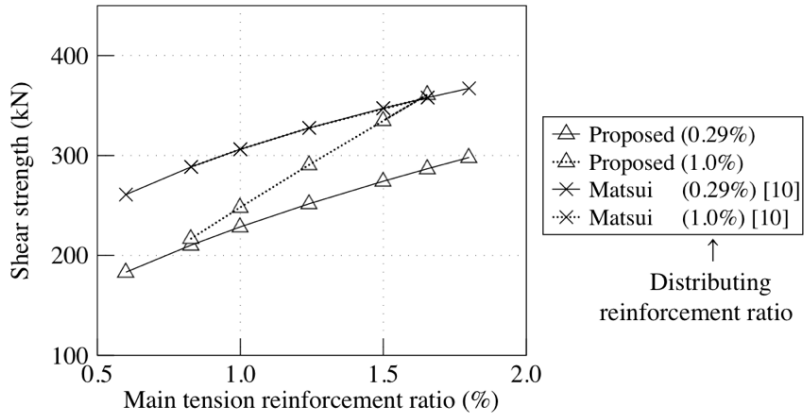

Fig. 10 – Relationships between shear strength and main reinforcement ratio

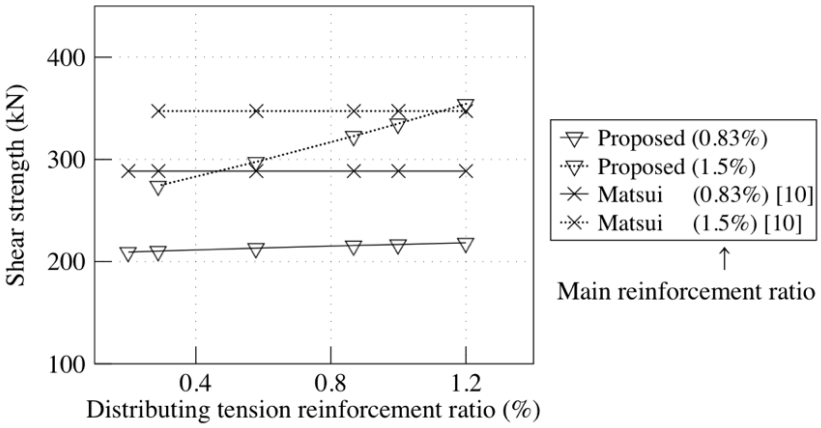

Fig. 11 – Relationships between shear strength and distributing reinforcement ratio

4.3 Influence of reinforcement on fatigue life

In the proposed method, distributing reinforcement were considered as a predominant factor for understanding fatigue life in addition to the main reinforcement. Therefore, we conducted FEA with varying main and distributing tension reinforcement ratios by using specimen RC39-7 as a reference. Specimen RC39-7 with the almost lowest reinforcement ratio is selected from among the experimental data as shown in section 2.1. Hence, in

the comparison, main and distributing reinforcement ratios are changed to 1.5–2 times and 2–3 times the default value, respectively. Those reinforcement ratios are still in the range of all experimental data given in section 2.1. Therefore, the selected reinforcement ratios are within the range of application for the proposed method.

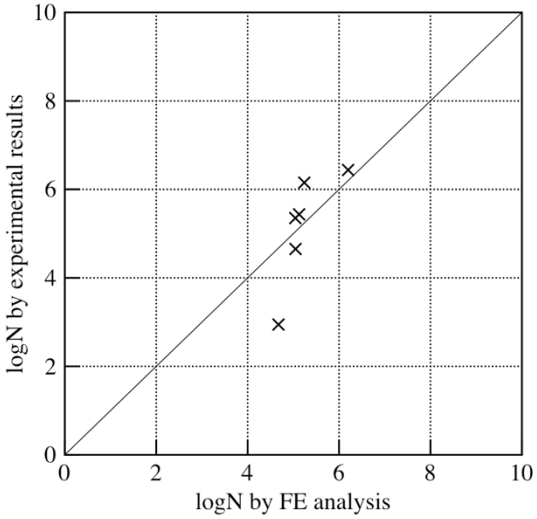

Fig. 12 – Comparison of fatigue life of experimental and FE analysis results

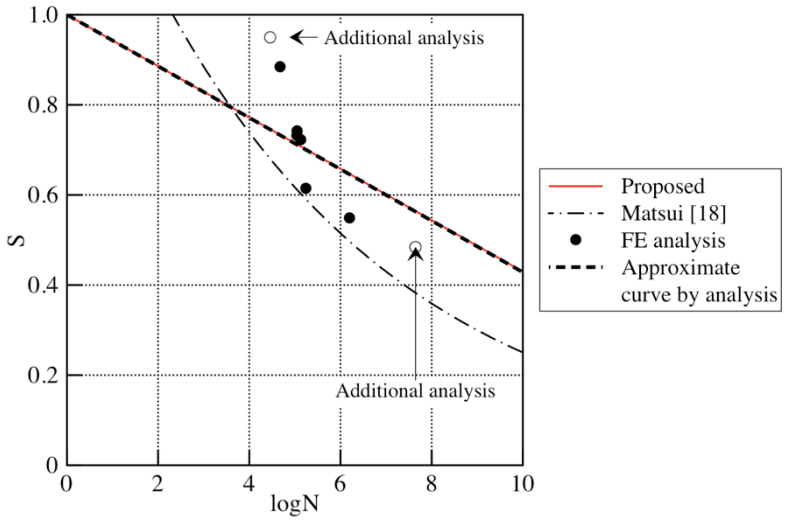

Fig. 13 – Predicted S–N curves and FE analysis results

Figures 14 and 15 show the influence of main and distributing tension reinforcement on fatigue life. The vertical axis and horizontal axis correspond to the ratio of the logarithmic fatigue life logN normalized by the fatigue life of a reference slab and main/distributing reinforcement ratio, respectively. An increase in the main reinforcement ratio evidently increases fatigue life in the proposed method and Matsui's equation. The FE analysis shows a low increment, such that the influence of the main reinforcement, is very low. When the distributing reinforcement ratio increases, Matsui's equation exhibits a constant fatigue life. The FEA expects a slightly higher fatigue life although it is a very low increment when compared with that of the proposed method.

Although the influences of reinforcement ratios in the proposed method are completely different from those of FEA and Matsui's equation, it should be noted that the proposed method comprehensively evaluates past experimental results, as shown in Figs. 2 through 5. A future study will involve extending the proposed method to predict the fatigue life of RC/PC slabs with stepped loading and performing a further comparison with results achieved in past studies.

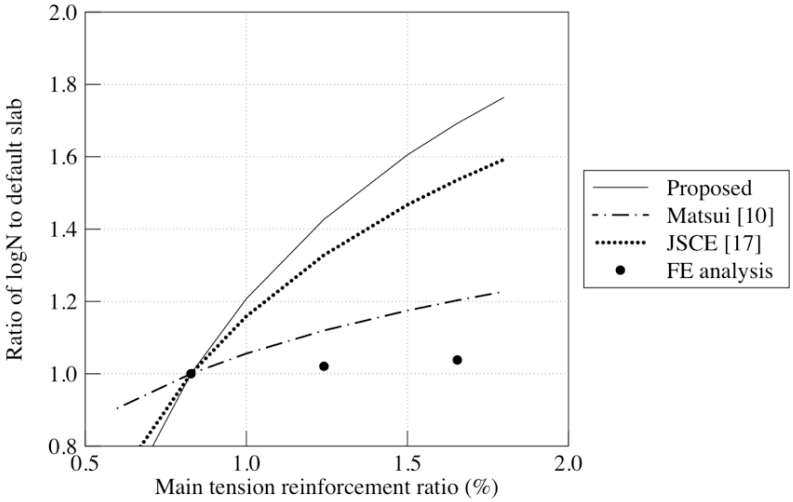

Fig. 14 – Influence of the main reinforcement on fatigue life

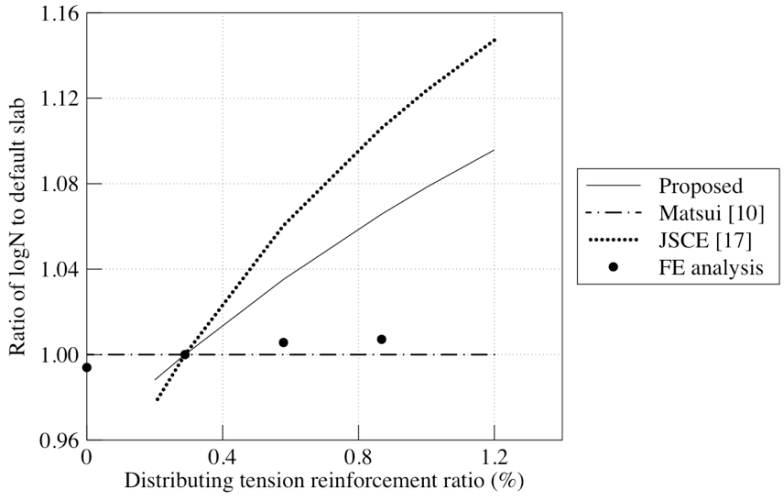

Fig. 15 – Influence of the distributing reinforcement on fatigue life

5. Conclusion

(1) RC slabs can be modeled as beam-formed member under a biaxial stress state because of both main and distributing reinforcement, which significantly affect the fatigue life of RC slabs, acting on the cross-section of longitudinal and transverse directions.

(2) A fatigue life prediction method was developed for RC slabs under a traveling wheel-type load based on JSCE shear design equation for a linear member. That can consider the influences of both main and distributing reinforcement.

(3) A comparative investigation of fatigue life between the proposed equation, the existing equation by Matsui and the 3D FE analysis revealed that the proposed equation was more sensitive to the influence of reinforcement.

Acknowledgements

A part of the present work was performed as a part of activities of Research Institute of Sustainable Future Society, Waseda Research Institute for Science and Engineering, Waseda University.

References

1. Takahashi, Y.; Tanaka, Y.; and Maekawa, K. (2016) "Multi-Scale Fatigue Simulations of RC Bridge Slabs Subjected to ASR Expansions", The 7th International Conference of Asian Concrete Federation, Hanoi, Vietnam.
2. Arora, V. V.; Singh, B.; and Yadav, L. (2016) "Flexural and Fatigue Behavior of Prestressed Concrete Beams Made with Portland Pozzolana Cement", Journal of Asian Concrete Federation, 2(1), pp. 15-23.
3. Graddy, J. C.; Kim, J.; Whitt, J. H.; Burns, N. H.; and Klingher, R. E. (2002) "Punching-Shear Behavior of Bridge Decks Under Fatigue

Loading", ACI Structural Journal, 99(3), pp.257-26.
4. Matsui, S. (1984) "Study on Fatigue and Design Method of Concrete Deck Slabs for Road Bridge", Doctoral thesis of Osaka University (*in Japanese*).
5. Kakuta, Y.; Itoh, A.; and Fujita, Y. (1974) "Experimental Study on Punching Strength of Reinforced Concrete Slabs", Proceedings of the Japan Society of Civil Engineers, 229, pp. 105-115 (*in Japanese*).
6. Kakuta, Y. and Fujita, Y. (1982) "Fatigue Strength of Reinforced Concrete Slabs Failing by Punching Shear", Proceedings of the Japan Society of Civil Engineers, 317, pp. 149-157 (*in Japanese*).
7. Abe, T.; Kida, T.; Takano, M.; and Kawai, Y. (2015) "Evaluation of the Punching Shear Strength and Fatigue Resistance of Road Bridge RC Slabs", JSCE Journal of structural engineering, 61A, pp. 39-54 (*in Japanese*).
8. Abe, T.; Kida, T.; Minakuchi, K.; and Kawai, Y. (2009) "Evaluation Formula for the Punching Shear Capacity of RC Slabs in Highway Bridges Under Running Loads", Journal of Structural Engineering, 55A, pp. 1468-1477(*in Japanese*).
9. Maeshima, T.; Koda, Y.; Tsuchiya, S.; and Iwaki, I. (2014) "Influence of Corrosion of Rebars Caused by Chloride Induced Deterioration on Fatigue Resistance in RC Road Bridge Deck", Journal of Japan Society of Civil Engineers, Ser. E2 (Materials and Concrete Structures), 70(2), pp. 208-225 (*in Japanese*).
10. Matsui, S. (1987) "Fatigue Strength of RC-Slabs of Highway Bridges by Wheel Running", Proceedings of the Japan Concrete Institute, 9(2), pp. 627-632 (*in Japanese*).
11. Boothby, T. E. and Laman, J. A. (1999) "Cumulative Damage to Bridge Concrete Deck Slabs Due to Vehicle Loading", ASCE Journal of Bridge Engineering, 4(1), pp. 80-82.
12. Maekawa, K.; Gebreyouhannes, E.; Mishima, T.; and An, X. (2006) "Three-Dimensional Fatigue Simulation of RC Slabs under Traveling Wheel-Type Loads", Journal of Advanced Concrete Technology, 4(3), pp. 445-457.
13. Fujiyama, C.; Gebreyouhannes, E.; Chijiwa, N.; and Maekawa, K. (2007) "Numerical Analysis of Various Factors on Fatigue Life for Slab under Moving Load", Proceedings of the Japan Concrete Institute, 29(3), pp. 727-732 (*in Japanese*).
14. Hiratsuka, Y.; Senda, M.; Fujiyama, C.; and Maekawa, K. (2016) "Fatigue-Based Structural Behavior of RC Bridge Slabs with Different Loading Histories", Journal of Japan Society of Civil Engineers, Ser. E2 (Materials and Concrete Structures), 72(4), pp. 323-342 (*in Japanese*).
15. Hiratsuka, Y. and Maekawa, K. (2016) "Serviceability Simulation of RC Bridge Decks Subjected to Coupled Drying Shrinkage and Wheel-Type Fatigue Loads", Journal of Japan Society of Civil Engineers, Ser. E2 (Materials and Concrete Structures), 72(4), pp.343-354 *(in Japanese*).
16. JSCE (2012), Proceeding of 7th Symposium on Decks of Highway Bridge, appendix, Japan.
17. JSCE (2013), Standard specification for concrete structures-2012, "Design", Japan.
18. Matsui, S. (1991) "Life Time Prediction of Bridges", Journal of Japan Society for Safety Engineering, 30(6), pp. 432-440 (*in Japanese*).